Spectral Overlap Method for Determining Resonances in Finite Continuum/on Lattice

Lukas Bovermann (lukas.bovermann@rub.de),
E. Epelbaum, H. Krebs, D. Lee
— NLEFT collaboration —

Institut für Theoretische Physik II
Ruhr-Universität Bochum

RUHR UNIVERSITÄT BOCHUM RUB

Workshop “Frontiers in Nuclear Physics”
(ERC AdG “EXOTIC”)

European Research Council
Established by the European Commission

Bethe Center for Theoretical Physics, Bonn, Germany
21-23 November 2023

Outline

Introduction

- S-matrix $S(k)$ can have resonance poles in lower complex half plane:

$$k_{\text{pole}} = k_0 - \mathrm{i}\kappa, \quad k_0 \in \mathbb{R}, \quad \kappa > 0$$

$$\Rightarrow E_{\text{pole}}^{\text{CMS}} = \frac{k_{\text{pole}}^2}{2\mu} = E_0 - \mathrm{i}\frac{\Gamma}{2} + \mathcal{O}(\kappa^2)$$

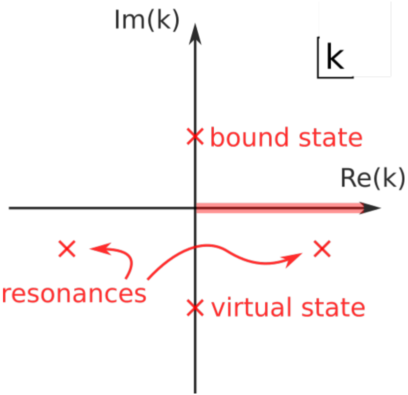

[I. Matuschek et al. (2021)]

- S-matrix $S(k)$ can have resonance poles in lower complex half plane:

$$k_{\text{pole}} = k_0 - \mathrm{i}\kappa, \quad k_0 \in \mathbb{R}, \quad \kappa > 0$$

$$\Rightarrow E_{\text{pole}}^{\text{CMS}} = \frac{k_{\text{pole}}^2}{2\mu} = E_0 - \mathrm{i}\frac{\Gamma}{2} + \mathcal{O}(\kappa^2)$$

- resonances also appear in cross section $\sigma(E \in \mathbb{R})$ as Breit-Wigner peaks with center and width roughly given by E_0 and Γ, respectively
  $\Rightarrow$ measurable in experiment

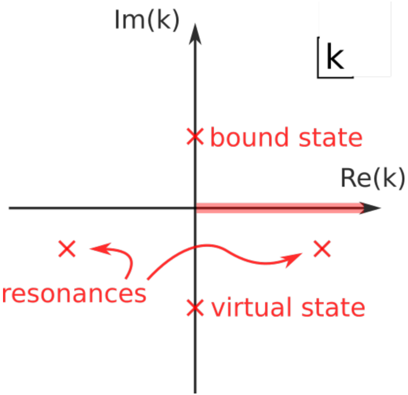

[I. Matuschek et al. (2021)]

Introduction

- S-matrix $S(k)$ can have resonance poles in lower complex half plane:

$$k_{\text{pole}} = k_0 - \mathrm{i}\kappa, \quad k_0 \in \mathbb{R}, \quad \kappa > 0$$

$$\Rightarrow E_{\text{pole}}^{\text{CMS}} = \frac{k_{\text{pole}}^2}{2\mu} = E_0 - \mathrm{i}\frac{\Gamma}{2} + \mathcal{O}(\kappa^2)$$

- resonances also appear in cross section $\sigma(E \in \mathbb{R})$ as Breit-Wigner peaks with center and width roughly given by E_0 and Γ, respectively
  $\Rightarrow$ measurable in experiment

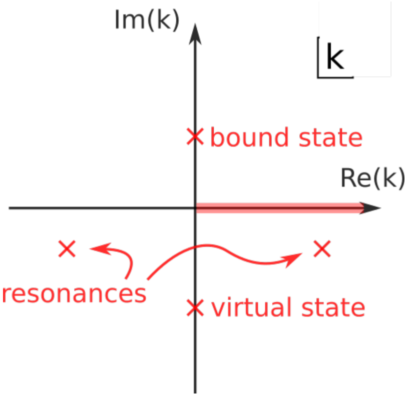

[I. Matuschek et al. (2021)]

- new method to determine E_0 and Γ with several advantages compared to Lüscher's formula

Method: Infinite continuum

- 1D benchmark: particle with reduced mass $\mu = m_\mathrm{N} = 938.92\ \mathrm{MeV}$ ("deuteron-deuteron scattering") in step-barrier potential

value for m_N from [B. Borasoy et al. (2007)]

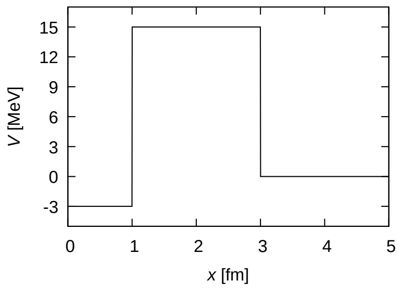

Method: Infinite continuum

- 1D benchmark: particle with reduced mass $\mu = m_\mathrm{N} = 938.92\ \mathrm{MeV}$ ("deuteron-deuteron scattering") in step-barrier potential

  value for m_N from [B. Borasoy et al. (2007)]

- solve CMS Schrödinger equation to obtain even-parity wave function with asymptotics

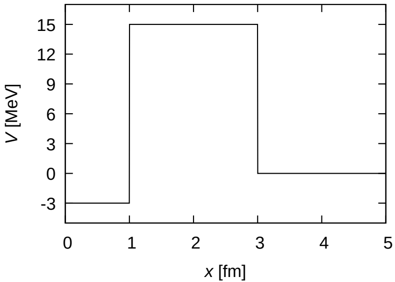

$$\psi(x \to \infty) = A \exp(-\mathrm{i}kx) + AS \exp(\mathrm{i}kx), \quad k = \sqrt{2\mu E}$$

Method: Infinite continuum

- 1D benchmark: particle with reduced mass $\mu = m_{\mathrm{N}} = 938.92\ \mathrm{MeV}$ ("deuteron-deuteron scattering") in step-barrier potential

  value for m_{N} from [B. Borasoy et al. (2007)]

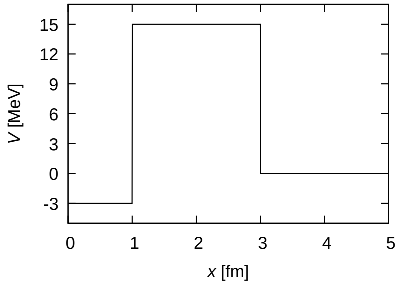

- solve CMS Schrödinger equation to obtain even-parity wave function with asymptotics

$$\psi(x \to \infty) = A \exp(-\mathrm{i}kx) + AS \exp(\mathrm{i}kx), \quad k = \sqrt{2\mu E}$$

- find pole of S-matrix numerically:

$$E_{\mathrm{pole}} = (7.1681 - 1.0484\mathrm{i})\ \mathrm{MeV}, \quad E_0 = 7.1681\ \mathrm{MeV}, \quad \Gamma = 2.0968\ \mathrm{MeV}$$

$\Rightarrow$ broad resonance near threshold to explore possibilities of method

Method: Infinite continuum

- calculate total cross section from S-matrix:

$$\sigma = 2\left|\frac{S-1}{2}\right|^2$$

(factor of 2 due to “angular integration”)

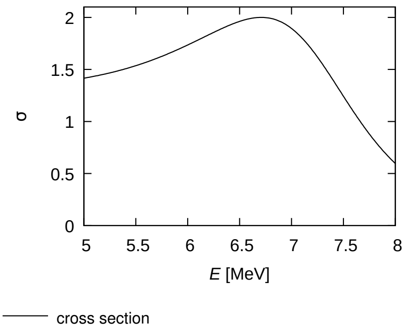

Method: Infinite continuum

- calculate total cross section from S-matrix:

$$\sigma = 2\left|\frac{S-1}{2}\right|^2$$

(factor of 2 due to “angular integration”)

- obtain Breit-Wigner peak from S-matrix pole:

$$\sigma\left(E \approx E_0 - \mathrm{i}\frac{\Gamma}{2}\right) \approx 2\frac{\Gamma^2/4}{(E-E_0)^2+\Gamma^2/4}$$

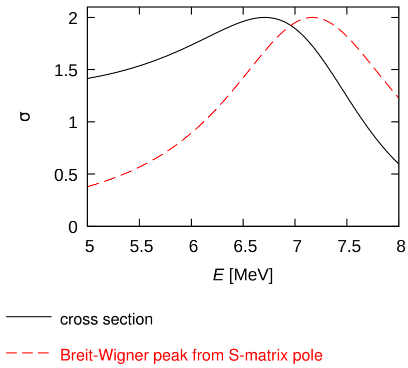

- discrepancy caused by broad resonance and non-vanishing background of σ

Method: Finite continuum

- enclose system in box of finite length, e.g. $L = 200\ \mathrm{fm}$:

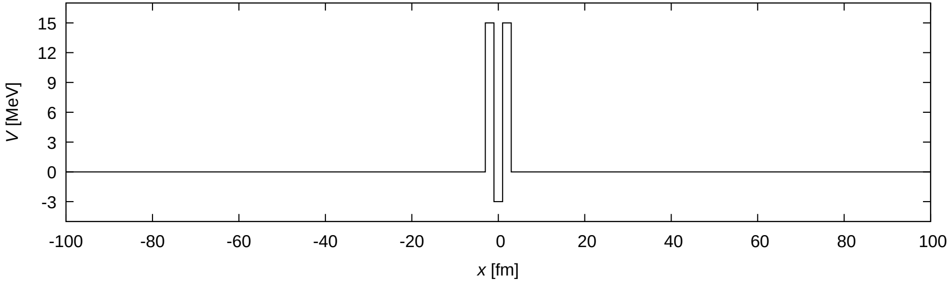

Method: Finite continuum

- enclose system in box of finite length, e.g. $L = 200$ fm:

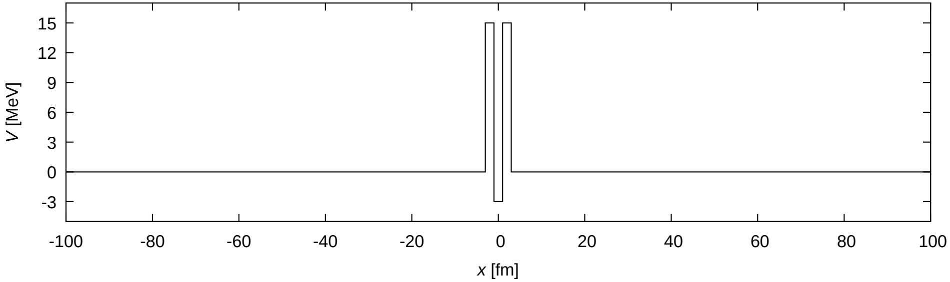

- impose periodic boundary conditions for even parity:

$$\psi(-L/2) = \psi(L/2), \quad \psi'(\pm L/2) = 0$$

Method: Finite continuum

- enclose system in box of finite length, e.g. $L = 200$ fm:

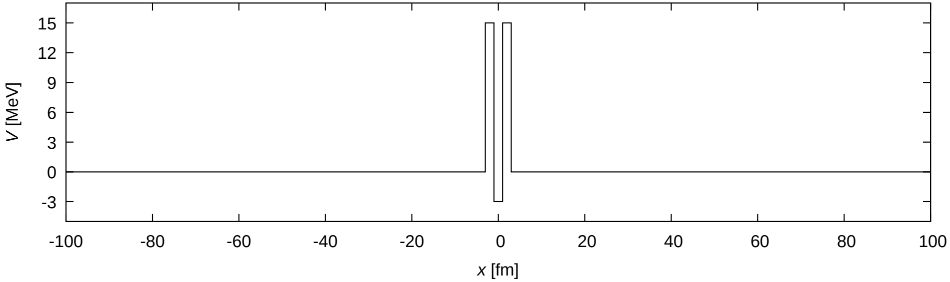

- impose periodic boundary conditions for even parity:

$$\psi(-L/2) = \psi(L/2), \quad \psi'(\pm L/2) = 0$$

⇒ states above threshold become discrete in energy and normalizable ($\int_{-L/2}^{L/2} \mathrm{d}x\, |\psi(x)|^2 = 1$)

Method: Finite continuum

- solve CMS Schrödinger equation to obtain even-parity wave function $\psi_E(x)$:

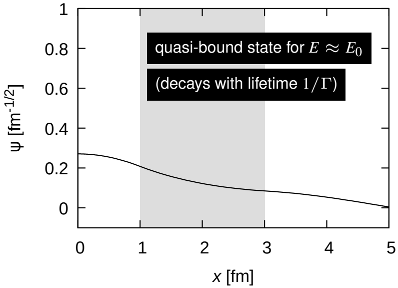

barrier

wave function

ψ_E

Method: Finite continuum

- solve CMS Schrödinger equation to obtain even-parity wave function $\psi_E(x)$:

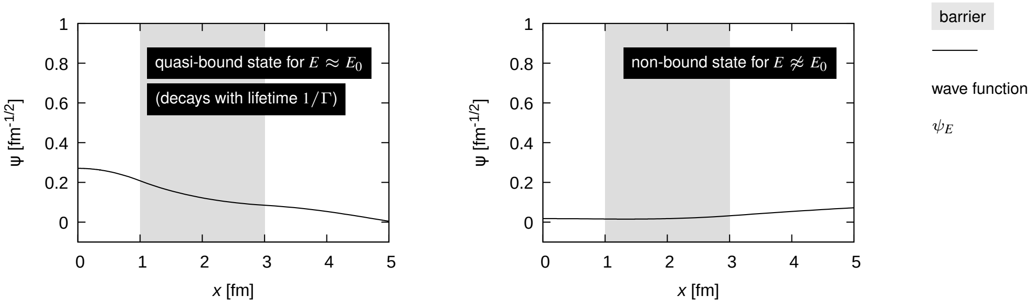

Method: Finite continuum

- solve CMS Schrödinger equation to obtain even-parity wave function $\psi_E(x)$:

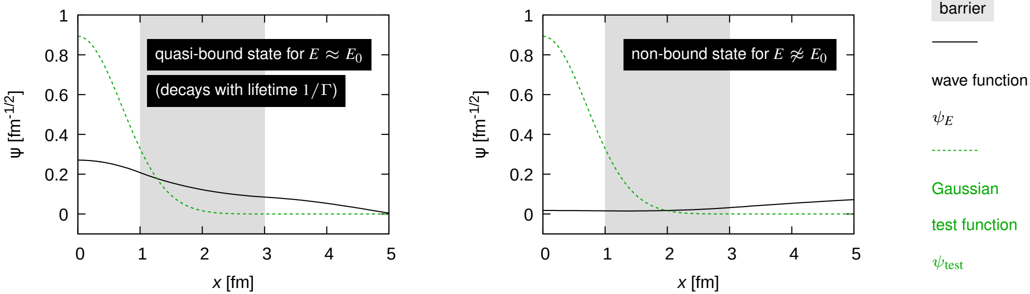

$\Rightarrow$ large overlap $\Rightarrow$ small overlap

- compute overlap $|\langle\psi_{\text{test}}|\psi_E\rangle|^2$ with Gaussian test function $\psi_{\text{test}}(x)$:

$$|\langle\psi_{\text{test}}|\psi_E\rangle|^2 = \left| \int_{-L/2}^{L/2} \mathrm{d}x\, \psi_{\text{test}}(x)\psi_E(x) \right|^2,$$

$$\psi_{\text{test}}(x) = \exp(-x^2/a_G^2)\Big/\sqrt{a_G\sqrt{\pi/2}\,\mathrm{erf}(L/(\sqrt{2}a_G))}, \quad a_G = 1\ \text{fm}$$

Method: Finite continuum

- plot spectral overlap function depending on energy $\Rightarrow$ must be peaked around E_0

Method: Finite continuum

- plot spectral overlap function depending on energy $\Rightarrow$ must be peaked around E_0

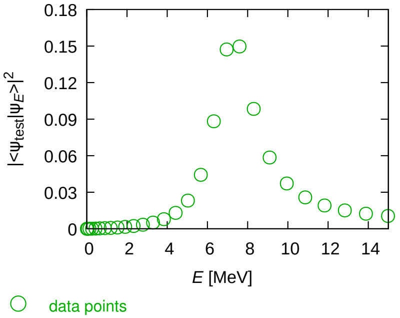

Method: Finite continuum

- plot spectral overlap function depending on energy $\Rightarrow$ must be peaked around E_0

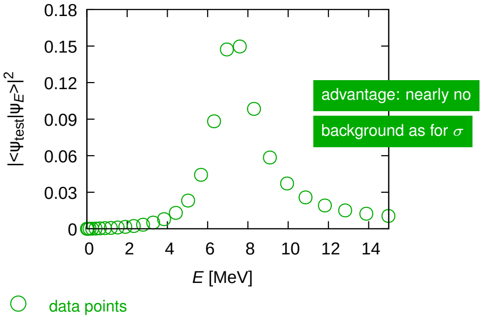

Method: Finite continuum

- plot spectral overlap function depending on energy $\Rightarrow$ must be peaked around E_0
- works if $|\psi_{\text{test}}\rangle \approx A|\psi_{E_0 - \mathrm{i}\Gamma/2}\rangle$ so that

$$|\langle\psi_{\text{test}}|e^{-\mathrm{i}\hat{H}\tau}|\psi_{\text{test}}\rangle|^2 \approx |A|^4 e^{-\Gamma t}$$

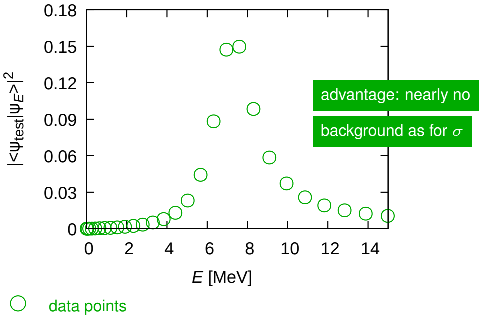

Method: Finite continuum

- plot spectral overlap function depending on energy $\Rightarrow$ must be peaked around E_0
- works if $|\psi_{\text{test}}\rangle \approx A|\psi_{E_0 - \mathrm{i}\Gamma/2}\rangle$ so that

$$|\langle\psi_{\text{test}}|e^{-\mathrm{i}\hat{H}\tau}|\psi_{\text{test}}\rangle|^2 \approx |A|^4 e^{-\Gamma t}$$

- expect Breit-Wigner shape to reproduce this proportionality (details on request):

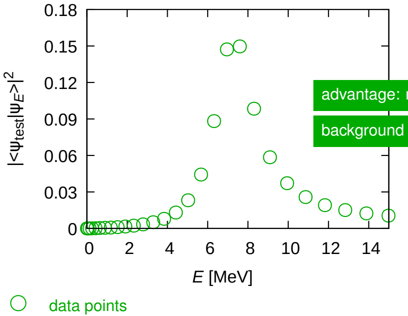

advantage: nearly no background as for σ

$$\langle\psi_{\text{test}}|\psi_E\rangle = \frac{\langle\psi_{\text{test}}|\psi_{E_0}\rangle\Gamma/2}{E - E_0 + \mathrm{i}\Gamma/2} \quad \Rightarrow \quad |\langle\psi_{\text{test}}|e^{-\mathrm{i}\hat{H}\tau}|\psi_{\text{test}}\rangle|^2 = \cdots \propto e^{-\Gamma t}$$

Method: Finite continuum

- plot spectral overlap function depending on energy $\Rightarrow$ must be peaked around E_0
- works if $|\psi_{\text{test}}\rangle \approx A|\psi_{E_0-\mathrm{i}\Gamma/2}\rangle$ so that

$$|\langle\psi_{\text{test}}|e^{-\mathrm{i}\hat{H}\tau}|\psi_{\text{test}}\rangle|^2 \approx |A|^4 e^{-\Gamma t}$$

- expect Breit-Wigner shape to reproduce this proportionality (details on request):

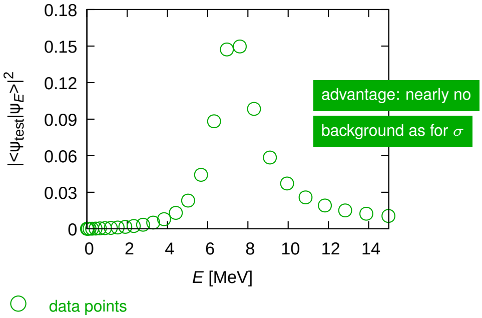

$$\langle\psi_{\text{test}}|\psi_E\rangle = \frac{\langle\psi_{\text{test}}|\psi_{E_0}\rangle\Gamma/2}{E - E_0 + \mathrm{i}\Gamma/2} \quad \Rightarrow \quad |\langle\psi_{\text{test}}|e^{-\mathrm{i}\hat{H}\tau}|\psi_{\text{test}}\rangle|^2 = \cdots \propto e^{-\Gamma t}$$

- fit Breit-Wigner peak to data (with 95 % fit errors):

$$|\langle\psi_{\text{test}}|\psi_E\rangle|^2 = |\langle\psi_{\text{test}}|\psi_{E_0}\rangle|^2 \frac{\Gamma^2/4}{(E-E_0)^2 + \Gamma^2/4} \quad \Rightarrow \begin{cases} E_0 = (7.4060 \pm 0.0864)\ \text{MeV}, \\ \Gamma = (2.3131 \pm 0.2438)\ \text{MeV} \end{cases}$$

Method: Finite continuum

- plot spectral overlap function depending on energy $\Rightarrow$ must be peaked around E_0
- works if $|\psi_{\text{test}}\rangle \approx A|\psi_{E_0 - \mathrm{i}\Gamma/2}\rangle$ so that

$$|\langle\psi_{\text{test}}|e^{-\mathrm{i}\hat{H}\tau}|\psi_{\text{test}}\rangle|^2 \approx |A|^4 e^{-\Gamma t}$$

- expect Breit-Wigner shape to reproduce this proportionality (details on request):

$$\langle\psi_{\text{test}}|\psi_E\rangle = \frac{\langle\psi_{\text{test}}|\psi_{E_0}\rangle\Gamma/2}{E - E_0 + \mathrm{i}\Gamma/2} \quad \Rightarrow \quad |\langle\psi_{\text{test}}|e^{-\mathrm{i}\hat{H}\tau}|\psi_{\text{test}}\rangle|^2 = \cdots \propto e^{-\Gamma t}$$

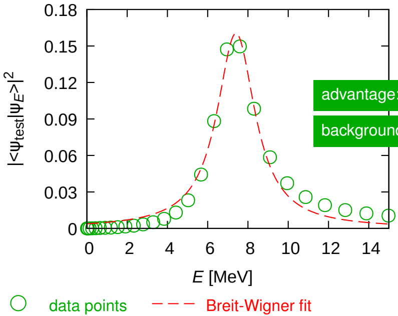

advantage: nearly no background as for σ

- fit Breit-Wigner peak to data (with 95 % fit errors):

$$|\langle\psi_{\text{test}}|\psi_E\rangle|^2 = |\langle\psi_{\text{test}}|\psi_{E_0}\rangle|^2 \frac{\Gamma^2/4}{(E - E_0)^2 + \Gamma^2/4} \quad \Rightarrow \begin{cases} E_0 = (7.4060 \pm 0.0864)\ \mathrm{MeV}, \\ \Gamma = (2.3131 \pm 0.2438)\ \mathrm{MeV} \end{cases}$$

Method: Finite continuum

- extrapolate in limit $L \to \infty$ by fitting $1/L$-expansion of $E_0(L)$, $\Gamma(L)$:

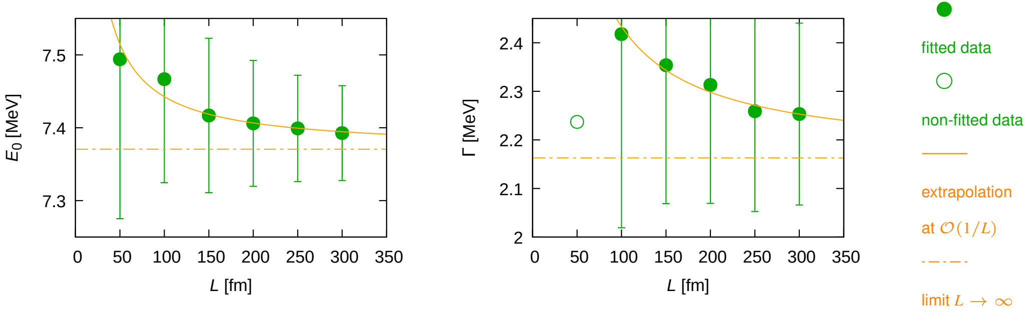

$\Rightarrow E_0/\mathrm{MeV} = 7.3706 \pm 0.2005$, $\Gamma/\mathrm{MeV} = 2.1629 \pm 0.9562$ (95 % extr. errors)

Method: Finite continuum

- extrapolate in limit $L \to \infty$ by fitting $1/L$-expansion of $E_0(L)$, $\Gamma(L)$:

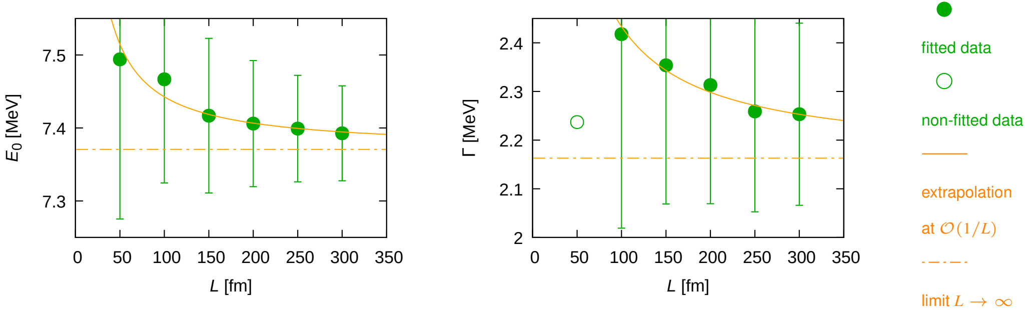

$\Rightarrow E_0/\mathrm{MeV} = 7.3706 \pm 0.2005$, $\Gamma/\mathrm{MeV} = 2.1629 \pm 0.9562$ (95 % extr. errors)

- vary width of Gaussian test function as $a_G \in \{0.5\ \mathrm{fm}, 1\ \mathrm{fm}, 1.5\ \mathrm{fm}\}$
  $\Rightarrow$ methodical error

Method: Finite continuum

- extrapolate in limit $L \to \infty$ by fitting $1/L$-expansion of $E_0(L)$, $\Gamma(L)$:

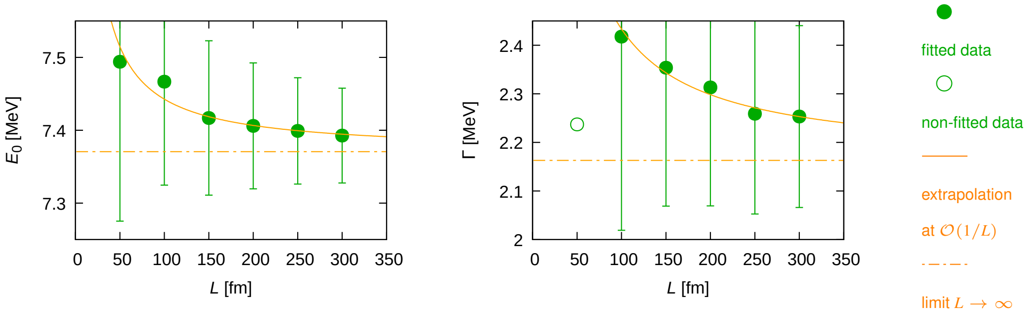

$\Rightarrow E_0/\mathrm{MeV} = 7.3706 \pm 0.2005$, $\Gamma/\mathrm{MeV} = 2.1629 \pm 0.9562$ (95 % extr. errors)

- vary width of Gaussian test function as $a_\mathrm{G} \in \{0.5\ \mathrm{fm}, 1\ \mathrm{fm}, 1.5\ \mathrm{fm}\}$
  $\Rightarrow$ methodical error
- combine all error sources (details on request):
  $E_0 = (7.3706^{+0.2477}_{-0.2183})$ MeV, $\Gamma = (2.1629^{+1.1075}_{-1.0347})$ MeV

Method: Finite continuum

- extrapolate in limit $L \to \infty$ by fitting $1/L$-expansion of $E_0(L)$, $\Gamma(L)$:

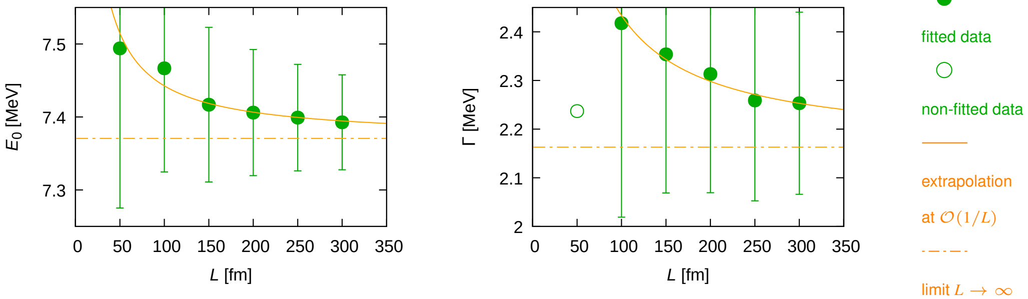

$\Rightarrow E_0/\mathrm{MeV} = 7.3706 \pm 0.2005$, $\Gamma/\mathrm{MeV} = 2.1629 \pm 0.9562$ (95 % extr. errors)

- vary width of Gaussian test function as $a_G \in \{0.5\ \mathrm{fm}, 1\ \mathrm{fm}, 1.5\ \mathrm{fm}\}$
  $\Rightarrow$ methodical error
- combine all error sources (details on request):
  $E_0 = (7.3706^{+0.2477}_{-0.2183})\ \mathrm{MeV}$, $\Gamma = (2.1629^{+1.1075}_{-1.0347})\ \mathrm{MeV}$

agrees with inf. cont. ✓

$E_0 = 7.1681\ \mathrm{MeV}$,
$\Gamma = 2.0968\ \mathrm{MeV}$

Method: Lattice (preliminary)

Method: Lattice (preliminary)

- introduce lattice with length $L = 1973.3$ fm & spacing $a = \frac{0.005}{\text{MeV}} = 0.98665$ fm:

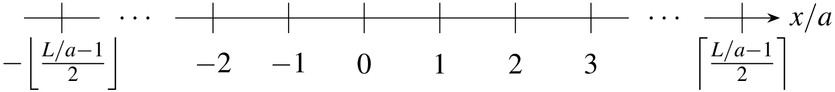

Method: Lattice (preliminary)

- introduce lattice with length $L = 1973.3\ \mathrm{fm}$ & spacing $a = \frac{0.005}{\mathrm{MeV}} = 0.98665\ \mathrm{fm}$:

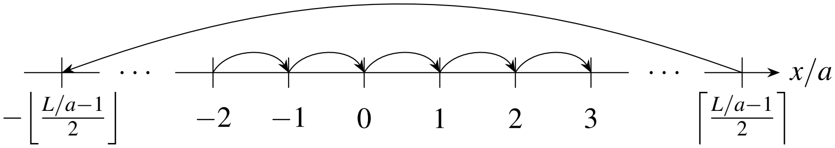

- require periodic boundary conditions: $\psi(x + nL) = \psi(x)\ \forall n \in \mathbb{Z}$

Method: Lattice (preliminary)

- introduce lattice with length $L = 1973.3$ fm & spacing $a = \frac{0.005}{\text{MeV}} = 0.98665$ fm:

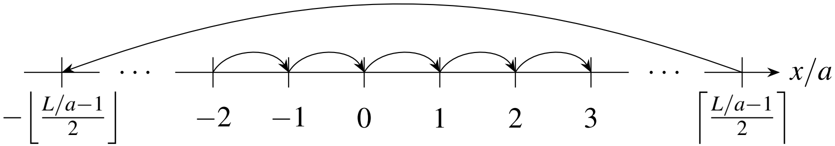

- require periodic boundary conditions: $\psi(x + nL) = \psi(x)\ \forall n \in \mathbb{Z}$
- discretize second derivative in kinetic-energy term: [D. Lee, R. Thomson (2007)]

$$
\begin{aligned}
\hat{H}\psi(x) = &\frac{49}{36\mu a^2}\psi(x) - \frac{3}{4\mu a^2}\Big(\psi(x-a) + \psi(x+a)\Big) \\
&+ \frac{3}{40\mu a^2}\Big(\psi(x-2a) + \psi(x+2a)\Big) - \frac{1}{180\mu a^2}\Big(\psi(x-3a) + \psi(x+3a)\Big) \\
&+ V(x)\psi(x)
\end{aligned}
$$

Method: Lattice (preliminary)

- step-barrier potential produces strong lattice artifacts

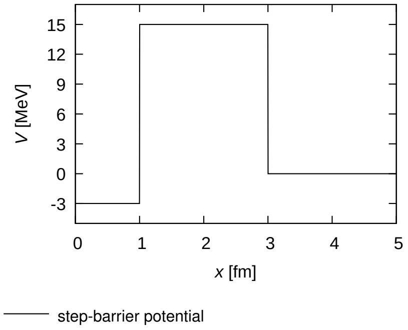

Method: Lattice (preliminary)

- step-barrier potential produces strong lattice artifacts ⇒ smooth it

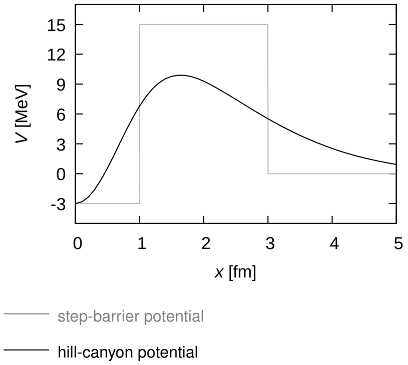

Method: Lattice (preliminary)

- step-barrier potential produces strong lattice artifacts $\Rightarrow$ smooth it
- compute eigenvalues E and eigenvectors $\langle x|\psi\rangle$ of Hamiltonian matrix $\langle x'|\hat{H}|x\rangle$ using Lanczos algorithm

  [C. Lanczos (1950)]

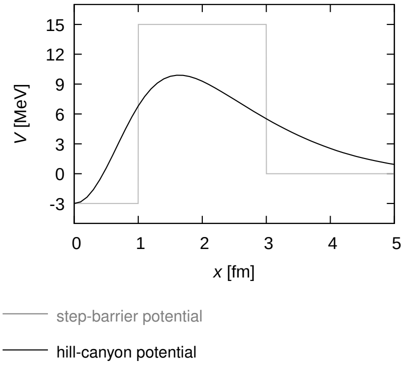

Method: Lattice (preliminary)

- step-barrier potential produces strong lattice artifacts $\Rightarrow$ smooth it
- compute eigenvalues E and eigenvectors $\langle x|\psi\rangle$ of Hamiltonian matrix $\langle x'|\hat{H}|x\rangle$ using Lanczos algorithm

  [C. Lanczos (1950)]
- select eigenvectors with even parity (no numerically unstable data at high E)

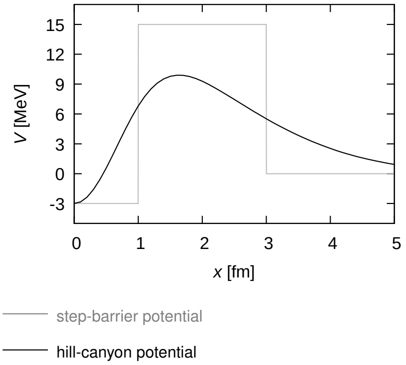

Method: Lattice (preliminary)

- step-barrier potential produces strong lattice artifacts $\Rightarrow$ smooth it
- compute eigenvalues E and eigenvectors $\langle x|\psi\rangle$ of Hamiltonian matrix $\langle x'|\hat{H}|x\rangle$ using Lanczos algorithm

  [C. Lanczos (1950)]
- select eigenvectors with even parity (no numerically unstable data at high E)
- calculate cross section from Lüscher's formula: [M. Lüscher (1986)]

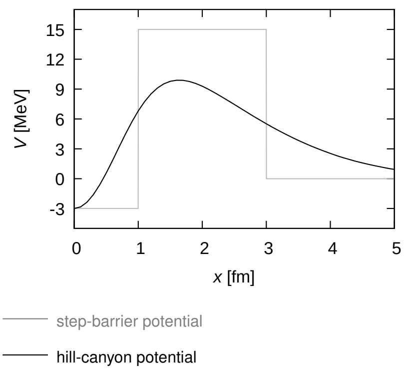

$$\sigma = 2\left|\frac{\exp(2i\delta)-1}{2}\right|^2, \quad \delta = -\frac{kL}{2}$$ via dispersion relation [D. Lee, R. Thomson (2007)]

$$E = \frac{49}{36\mu a^2} - \frac{3}{2\mu a^2}\cos(ka) + \frac{3}{20\mu a^2}\cos(2ka) - \frac{1}{90\mu a^2}\cos(3ka) = \frac{k^2}{2\mu} + \mathcal{O}(a^6)$$

Method: Lattice (preliminary) – Lüscher

- fit Breit-Wigner peak to Lüscher cross section (check $\sigma(E_0) = 2$):

$$\sigma(E) = \sigma(E_0)\frac{\Gamma^2/4}{(E-E_0)^2+\Gamma^2/4} \quad \Rightarrow \quad \begin{cases} E_0 = 6.2949 \text{ MeV}, \quad \Gamma = 3.0615 \text{ MeV}, \\ \sigma(E_0) = 2.0000 \ \checkmark \end{cases}$$

Method: Lattice (preliminary) – Lüscher

- fit Breit-Wigner peak to Lüscher cross section (check $\sigma(E_0) = 2$):

$$\sigma(E) = \sigma(E_0)\frac{\Gamma^2/4}{(E-E_0)^2+\Gamma^2/4} \quad \Rightarrow \quad \begin{cases} E_0 = 6.2949\ \text{MeV}, \quad \Gamma = 3.0615\ \text{MeV}, \\ \sigma(E_0) = 2.0000\ \checkmark \end{cases}$$

- extrapolate in limit $a \to 0$ by fitting a^2-expansion of $E_0(a)$, $\Gamma(a)$:

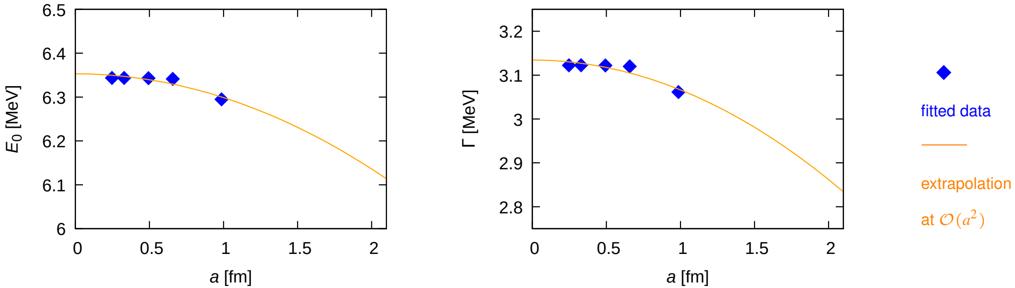

$\Rightarrow E_0/\text{MeV} = 6.3530 \pm 0.0186$, $\Gamma/\text{MeV} = 3.1345 \pm 0.0235$ (95 % extr. errors)

Method: Lattice (preliminary) – Lüscher vs. overlap

$E_0/\mathrm{MeV} = 6.3530 \pm 0.0186$, $\Gamma/\mathrm{MeV} = 3.1345 \pm 0.0235$ (95 % extr. errors)

- but for small and coarse lattices ($L \in \{17.760\ \mathrm{fm}, 21.706\ \mathrm{fm}\}$, $a = 1.9733\ \mathrm{fm}$):

Method: Lattice (preliminary) – Lüscher vs. overlap

$E_0/\text{MeV} = 6.3530 \pm 0.0186$, $\Gamma/\text{MeV} = 3.1345 \pm 0.0235$ (95 % extr. errors)

- but for small and coarse lattices ($L \in \{17.760\text{ fm}, 21.706\text{ fm}\}$, $a = 1.9733\text{ fm}$):

Lüscher's formula

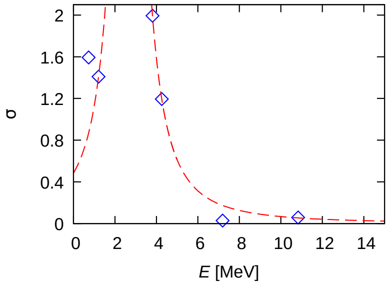

$\Rightarrow E_0 = 2.6572\text{ MeV},$
$\Gamma = 1.4233\text{ MeV},$
$\sigma(E_0) = 7.2325$ ↯

Method: Lattice (preliminary) – Lüscher vs. overlap

$E_0/\text{MeV} = 6.3530 \pm 0.0186$, $\Gamma/\text{MeV} = 3.1345 \pm 0.0235$ (95 % extr. errors)

- but for small and coarse lattices ($L \in \{17.760 \text{ fm}, 21.706 \text{ fm}\}$, $a = 1.9733$ fm):

Lüscher's formula	overlap method
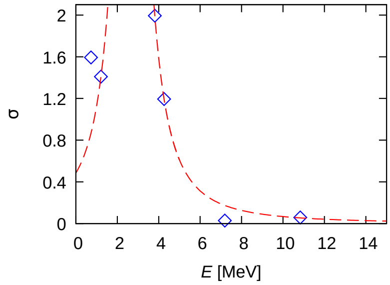	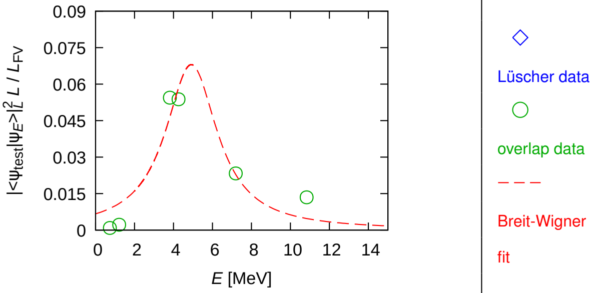
$\Rightarrow E_0 = 2.6572$ MeV, $\Gamma = 1.4233$ MeV, $\sigma(E_0) = 7.2325$ ↯	$\Rightarrow E_0 = 4.9136$ MeV, $\Gamma = 3.2428$ MeV, $\lvert\langle\psi_{\text{test}}\lvert\psi_{E_0}\rangle\rvert^2 = 0.068012$ ✓

Method: Lattice (preliminary) – Lüscher vs. overlap

- advantage: overlap has nearly no background like cross section

Method: Lattice (preliminary) – Lüscher vs. overlap

- advantage: overlap has nearly no background like cross section
- used Gaussian test function with width $a_{\mathrm{G}} = 1\ \mathrm{fm}$
  $\Rightarrow$ normalized it in same way as eigenvectors of $\hat{H}$

Method: Lattice (preliminary) – Lüscher vs. overlap

- advantage: overlap has nearly no background like cross section
- used Gaussian test function with width $a_{\mathrm{G}} = 1\ \mathrm{fm}$
  $\Rightarrow$ normalized it in same way as eigenvectors of $\hat{H}$
- caution: $|\langle\psi_{\mathrm{test}}|\psi_E\rangle|_L^2 \propto L^{-1}$ is probability distributed over lattice length!

$$\frac{|\langle\psi_{\mathrm{test}}|\psi_E\rangle|_{L_1}^2}{|\langle\psi_{\mathrm{test}}|\psi_E\rangle|_{L_2}^2} = \frac{L_2}{L_1}$$

$\Rightarrow$ rescaled spectral overlap functions to $L_{\mathrm{FV}} = 200\ \mathrm{fm}$ (only works in 1D)

Method: Lattice (preliminary) – Lüscher vs. overlap

- advantage: overlap has nearly no background like cross section
- used Gaussian test function with width $a_{\mathrm{G}} = 1\ \mathrm{fm}$
  $\Rightarrow$ normalized it in same way as eigenvectors of $\hat{H}$
- caution: $|\langle\psi_{\mathrm{test}}|\psi_E\rangle|_L^2 \propto L^{-1}$ is probability distributed over lattice length!

$$\frac{|\langle\psi_{\mathrm{test}}|\psi_E\rangle|_{L_1}^2}{|\langle\psi_{\mathrm{test}}|\psi_E\rangle|_{L_2}^2} = \frac{L_2}{L_1}$$

  $\Rightarrow$ rescaled spectral overlap functions to $L_{\mathrm{FV}} = 200\ \mathrm{fm}$ (only works in 1D)
- uncertainty from averaging data for multiple lattice lengths not yet estimated

$$L \overset{?}{\approx} \frac{17.760\ \mathrm{fm} + 21.706\ \mathrm{fm}}{2} = 19.733\ \mathrm{fm}$$

(Lüscher's formula advantageously yields infinite-volume results)

Method: Lattice (preliminary) – overlap

- repeat simulation for $L/\mathrm{fm} \in \{\sim 50, \sim 100, \ldots, \sim 300\}$ and extrapolate $L \to \infty$

Method: Lattice (preliminary) – overlap

- repeat simulation for $L/\mathrm{fm} \in \{\sim 50, \sim 100, \ldots, \sim 300\}$ and extrapolate $L \to \infty$
- repeat simulation for different a-values and extrapolate $a \to 0$:

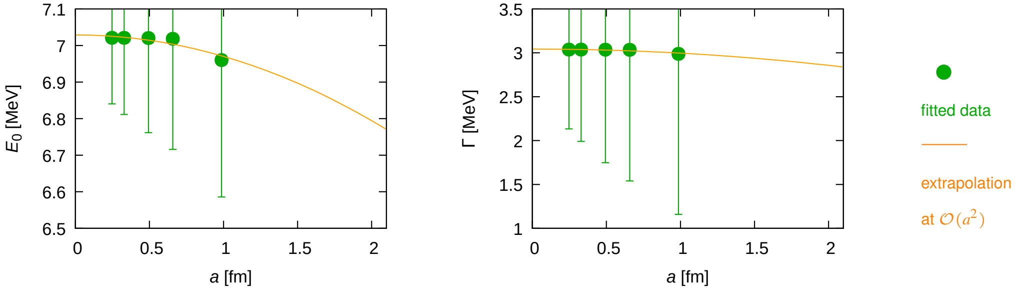

Method: Lattice (preliminary) – overlap

- repeat simulation for $L/\mathrm{fm} \in \{\sim 50, \sim 100, \ldots, \sim 300\}$ and extrapolate $L \to \infty$
- repeat simulation for different a-values and extrapolate $a \to 0$:

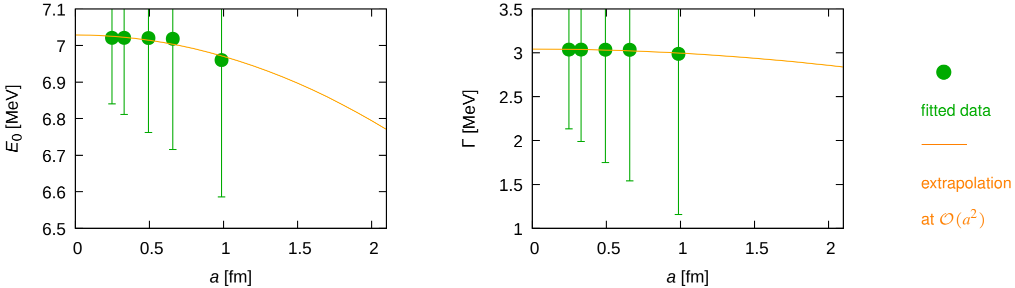

- repeat simulation for $a_\mathrm{G}/\mathrm{fm} \in \{0.75, 1, 1.25\}$ to determine methodical error

Method: Lattice (preliminary) – overlap

- repeat simulation for $L/\mathrm{fm} \in \{\sim 50, \sim 100, \ldots, \sim 300\}$ and extrapolate $L \to \infty$
- repeat simulation for different a-values and extrapolate $a \to 0$:

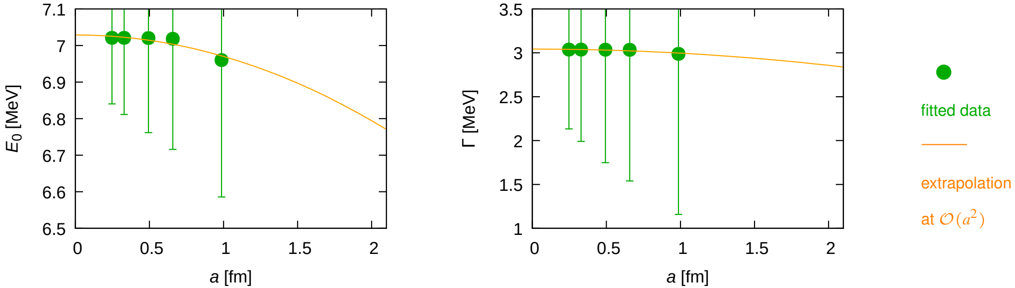

- repeat simulation for $a_{\mathrm{G}}/\mathrm{fm} \in \{0.75, 1, 1.25\}$ to determine methodical error
- combine BW-fit, extrapolation & methodical errors:
$E_0 = (7.0289^{+0.6586}_{-0.5519})\ \mathrm{MeV},\ \Gamma = (3.0429^{+3.1135}_{-2.9350})\ \mathrm{MeV}$

Method: Lattice (preliminary) – overlap

- repeat simulation for $L/\mathrm{fm} \in \{\sim 50, \sim 100, \ldots, \sim 300\}$ and extrapolate $L \to \infty$
- repeat simulation for different a-values and extrapolate $a \to 0$:

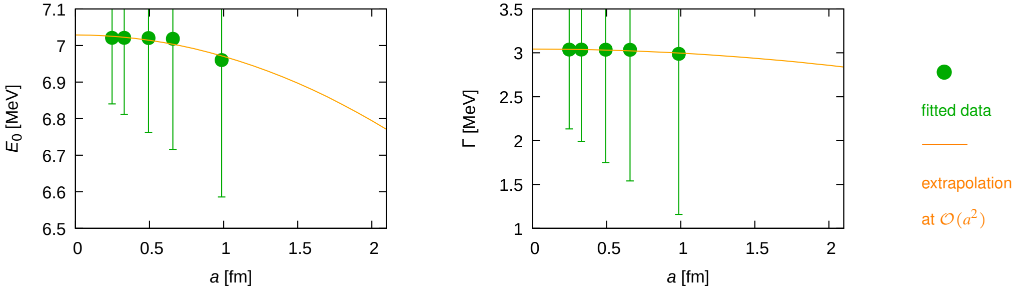

- repeat simulation for $a_G/\mathrm{fm} \in \{0.75, 1, 1.25\}$ to determine methodical error
- combine BW-fit, extrapolation & methodical errors:
  $E_0 = (7.0289^{+0.6586}_{-0.5519})$ MeV, $\Gamma = (3.0429^{+3.1135}_{-2.9350})$ MeV
- comparison: Lüscher error still underestimated

Lüscher results (no fit error)

$E_0/\mathrm{MeV} = 6.3530 \pm 0.0186,$
$\Gamma/\mathrm{MeV} = 3.1345 \pm 0.0235$

Outlook: From 1D to 3D

Outlook: From 1D to 3D

- generalize lattice Hamiltonian to three dimensions and non-zero spin: [B. Borasoy et al. (2007)]

$$\hat{H}|\vec{r}\rangle = -\frac{1}{2\mu}\left(\frac{\partial^2}{\partial x^2}+\frac{\partial^2}{\partial y^2}+\frac{\partial^2}{\partial z^2}\right)_{\text{discretized}}|\vec{r}\rangle + V(\vec{r},\hat{\vec{S}}_1,\hat{\vec{S}}_2)|\vec{r}\rangle$$

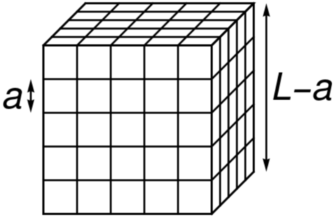

Outlook: From 1D to 3D

- generalize lattice Hamiltonian to three dimensions and non-zero spin: [B. Borasoy et al. (2007)]

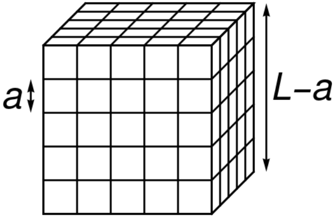

$$\hat{H}|\vec{r}\rangle = -\frac{1}{2\mu}\left(\frac{\partial^2}{\partial x^2}+\frac{\partial^2}{\partial y^2}+\frac{\partial^2}{\partial z^2}\right)_{\text{discretized}}|\vec{r}\rangle + V(\vec{r},\hat{\vec{S}}_1,\hat{\vec{S}}_2)|\vec{r}\rangle$$

- define radial states for partial wave ${}^{2s+1}l_j$ (easier for high l and partial-wave mixing than Lüscher's formula): [B.-N. Lu et al. (2016)] [B. Borasoy et al. (2007)]

$$|R\rangle_{s,l,j} = \sum_{\vec{r}}\sum_{l_z,s_z}\sum_{s_{z,1}}\sum_{s_{z,2}} C^{j,l,s}_{0,l_z,s_z} C^{s,s_1,s_2}_{s_z,s_{z,1},s_{z,2}} Y_{l,l_z}(\vec{e}_r)\delta_{r,R}|\vec{r}\rangle \otimes |s_{z,1},s_{z,2}\rangle$$

Outlook: From 1D to 3D

- generalize lattice Hamiltonian to three dimensions and non-zero spin: [B. Borasoy et al. (2007)]

$$\hat{H}|\vec{r}\rangle = -\frac{1}{2\mu}\left(\frac{\partial^2}{\partial x^2}+\frac{\partial^2}{\partial y^2}+\frac{\partial^2}{\partial z^2}\right)_{\text{discretized}}|\vec{r}\rangle + V(\vec{r},\hat{\vec{S}}_1,\hat{\vec{S}}_2)|\vec{r}\rangle$$

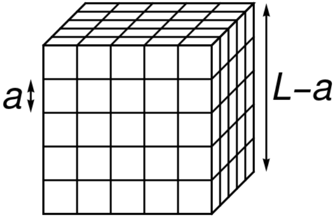

- define radial states for partial wave ${}^{2s+1}l_j$ (easier for high l and partial-wave mixing than Lüscher's formula): [B.-N. Lu et al. (2016)] [B. Borasoy et al. (2007)]

$$|R\rangle_{s,l,j} = \sum_{\vec{r}}\sum_{l_z,s_z}\sum_{s_{z,1}}\sum_{s_{z,2}} C^{j,l,s}_{0,l_z,s_z} C^{s,s_1,s_2}_{s_z,s_{z,1},s_{z,2}} Y_{l,l_z}(\vec{e}_r)\delta_{r,R}|\vec{r}\rangle \otimes |s_{z,1},s_{z,2}\rangle$$

- consider n coupled scattering channels, i.e. ${}_{\alpha'}\langle R'|V|R\rangle_\alpha$ is full $n \times n$ block:

$$|R\rangle_\alpha := |R\rangle_{s_\alpha,l_\alpha,j_\alpha} \quad \text{for} \quad \alpha \in \{1,\ldots,n\}$$

Outlook: From 1D to 3D

- add spherical wall potential [J. Carlson et al. (1984)] to avoid artifacts caused by periodic boundary condition:

$$V_{\mathrm{wall}}(\vec{r}) = \Lambda\theta(r - R_{\mathrm{wall}}), \quad \Lambda \text{ positive and large}$$

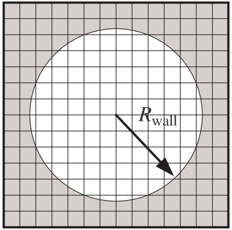

[B. Borasoy et al. (2007)]

Outlook: From 1D to 3D

- add spherical wall potential [J. Carlson et al. (1984)] to avoid artifacts caused by periodic boundary condition:

$$V_{\text{wall}}(\vec{r}) = \Lambda\theta(r - R_{\text{wall}}), \quad \Lambda \text{ positive and large}$$

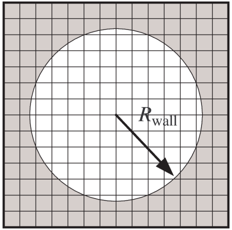

[B. Borasoy et al. (2007)]

- compute norm matrix $[N(R)]_{\alpha',\alpha} = {}_{\alpha'}\langle R|R\rangle_{\alpha}$ and project Hamiltonian onto normalized radial states:

$$[H_{\text{rad}}(R',R)]_{\alpha',\alpha} = \sum_{\beta,\beta'=1}^{n} [N^{-1/2}(R')]_{\alpha',\beta'}\,{}_{\beta'}\langle R'|(\hat{H} + V_{\text{wall}})|R\rangle_{\beta}[N^{-1/2}(R)]_{\beta,\alpha}$$

Outlook: From 1D to 3D

- add spherical wall potential [J. Carlson et al. (1984)] to avoid artifacts caused by periodic boundary condition:

$$V_{\text{wall}}(\vec{r}) = \Lambda\theta(r - R_{\text{wall}}), \quad \Lambda \text{ positive and large}$$

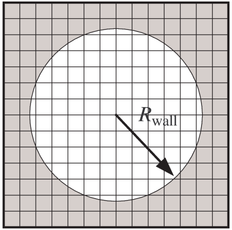

[B. Borasoy et al. (2007)]

- compute norm matrix $[N(R)]_{\alpha',\alpha} = {}_{\alpha'}\langle R|R\rangle_{\alpha}$ and project Hamiltonian onto normalized radial states:

$$[H_{\text{rad}}(R', R)]_{\alpha',\alpha} = \sum_{\beta,\beta'=1}^{n} [N^{-1/2}(R')]_{\alpha',\beta'} \, {}_{\beta'}\langle R'|(\hat{H} + V_{\text{wall}})|R\rangle_{\beta} [N^{-1/2}(R)]_{\beta,\alpha}$$

- obtain wave functions from eigenvectors $|\psi\rangle$ of H_{rad}:

$$\psi_{\alpha}(R) = \sum_{\beta=1}^{n} [N^{-1/2}(R)]_{\alpha,\beta} \, {}_{\beta}\langle R|\psi\rangle$$

Outlook: From 1D to 3D

- guess: n linearly independent solutions of Schrödinger equation needed to get full-rank $n \times n$ overlap matrix

Outlook: From 1D to 3D

- guess: n linearly independent solutions of Schrödinger equation needed to get full-rank $n \times n$ overlap matrix
- extended Schrödinger eq. in two-channel case (e.g. $^3\mathrm{SD}_1$): [B.-N. Lu et al. (2016)]

$$\begin{pmatrix} [H_{\mathrm{rad}}]_{1,1} & 0 & [H_{\mathrm{rad}}]_{1,2} & -U_0\delta_{r,R_{\mathrm{mix}}} \\ 0 & [H_{\mathrm{rad}}]_{1,1} & U_0\delta_{r,R_{\mathrm{mix}}} & [H_{\mathrm{rad}}]_{1,2} \\ [H_{\mathrm{rad}}]_{2,1} & U_0\delta_{r,R_{\mathrm{mix}}} & [H_{\mathrm{rad}}]_{2,2} & 0 \\ -U_0\delta_{r,R_{\mathrm{mix}}} & [H_{\mathrm{rad}}]_{2,1} & 0 & [H_{\mathrm{rad}}]_{2,2} \end{pmatrix} \begin{pmatrix} \psi_1(r) \\ \psi_2(r) \\ \chi_1(r) \\ \chi_2(r) \end{pmatrix} = E \begin{pmatrix} \psi_1(r) \\ \psi_2(r) \\ \chi_1(r) \\ \chi_2(r) \end{pmatrix}$$

mixing potential with $R_{\mathrm{mix}} \lesssim R_{\mathrm{wall}}$ and small U_0 varies initial conditions for H_{rad}

Outlook: From 1D to 3D

- guess: n linearly independent solutions of Schrödinger equation needed to get full-rank $n \times n$ overlap matrix
- extended Schrödinger eq. in two-channel case (e.g. $^3\mathrm{SD}_1$): **[B.-N. Lu et al. (2016)]**

$$\begin{pmatrix} [H_\mathrm{rad}]_{1,1} & 0 & [H_\mathrm{rad}]_{1,2} & -U_0\delta_{r,R_\mathrm{mix}} \\ 0 & [H_\mathrm{rad}]_{1,1} & U_0\delta_{r,R_\mathrm{mix}} & [H_\mathrm{rad}]_{1,2} \\ [H_\mathrm{rad}]_{2,1} & U_0\delta_{r,R_\mathrm{mix}} & [H_\mathrm{rad}]_{2,2} & 0 \\ -U_0\delta_{r,R_\mathrm{mix}} & [H_\mathrm{rad}]_{2,1} & 0 & [H_\mathrm{rad}]_{2,2} \end{pmatrix} \begin{pmatrix} \psi_1(r) \\ \psi_2(r) \\ \chi_1(r) \\ \chi_2(r) \end{pmatrix} = E \begin{pmatrix} \psi_1(r) \\ \psi_2(r) \\ \chi_1(r) \\ \chi_2(r) \end{pmatrix}$$

mixing potential with $R_\mathrm{mix} \lesssim R_\mathrm{wall}$ and small U_0 varies initial conditions for H_rad

- decomposition of 2×2 overlap matrix (cf. **[J. M. Blatt, L. C. Biedenharn (1952)]**):

$$\begin{pmatrix} |\langle\psi_\mathrm{test}|\psi_1\rangle|^2 & |\langle\psi_\mathrm{test}|\chi_1\rangle|^2 \\ |\langle\psi_\mathrm{test}|\psi_2\rangle|^2 & |\langle\psi_\mathrm{test}|\chi_2\rangle|^2 \end{pmatrix} = U^\dagger \begin{pmatrix} \cdot & 0 \\ 0 & \cdot \end{pmatrix} U, \quad U^\dagger U = \begin{pmatrix} 1 & 0 \\ 0 & 1 \end{pmatrix}$$

Outlook: From 1D to 3D

- guess: n linearly independent solutions of Schrödinger equation needed to get full-rank $n \times n$ overlap matrix
- extended Schrödinger eq. in two-channel case (e.g. ${}^3\mathrm{SD}_1$): **[B.-N. Lu et al. (2016)]**

$$\begin{pmatrix} [H_{\mathrm{rad}}]_{1,1} & 0 & [H_{\mathrm{rad}}]_{1,2} & -U_0\delta_{r,R_{\mathrm{mix}}} \\ 0 & [H_{\mathrm{rad}}]_{1,1} & U_0\delta_{r,R_{\mathrm{mix}}} & [H_{\mathrm{rad}}]_{1,2} \\ [H_{\mathrm{rad}}]_{2,1} & U_0\delta_{r,R_{\mathrm{mix}}} & [H_{\mathrm{rad}}]_{2,2} & 0 \\ -U_0\delta_{r,R_{\mathrm{mix}}} & [H_{\mathrm{rad}}]_{2,1} & 0 & [H_{\mathrm{rad}}]_{2,2} \end{pmatrix} \begin{pmatrix} \psi_1(r) \\ \psi_2(r) \\ \chi_1(r) \\ \chi_2(r) \end{pmatrix} = E \begin{pmatrix} \psi_1(r) \\ \psi_2(r) \\ \chi_1(r) \\ \chi_2(r) \end{pmatrix}$$

mixing potential with $R_{\mathrm{mix}} \lesssim R_{\mathrm{wall}}$ and small U_0 varies initial conditions for H_{rad}

- decomposition of 2×2 overlap matrix (cf. **[J. M. Blatt, L. C. Biedenharn (1952)]**):

$$\begin{pmatrix} |\langle\psi_{\mathrm{test}}|\psi_1\rangle|^2 & |\langle\psi_{\mathrm{test}}|\chi_1\rangle|^2 \\ |\langle\psi_{\mathrm{test}}|\psi_2\rangle|^2 & |\langle\psi_{\mathrm{test}}|\chi_2\rangle|^2 \end{pmatrix} = U^\dagger \begin{pmatrix} \cdot & 0 \\ 0 & \cdot \end{pmatrix} U, \quad U^\dagger U = \begin{pmatrix} 1 & 0 \\ 0 & 1 \end{pmatrix}$$

- generalization to $n > 2$ channels straightforward **[LB et al. (2019)]**

Outlook: (In)elastic nuclear scattering

- chiral lattice EFT calculations for many nucleons are performed as Monte-Carlo simulations (instead of using Lanczos algorithm)

Outlook: (In)elastic nuclear scattering

- chiral lattice EFT calculations for many nucleons are performed as Monte-Carlo simulations (instead of using Lanczos algorithm)

$\Rightarrow$ evolve Hamiltonian in Euclidean (i.e. Wick-rotated) time τ

Outlook: (In)elastic nuclear scattering

- chiral lattice EFT calculations for many nucleons are performed as Monte-Carlo simulations (instead of using Lanczos algorithm)

$\Rightarrow$ evolve Hamiltonian in Euclidean (i.e. Wick-rotated) time τ

$\Rightarrow$ evaluate matrix element $|\langle\psi_{\text{test}}|\exp(-\hat{H}\tau)|\psi_{\text{test}}\rangle|^2$ at different points in time to obtain spectral overlap function

Outlook: (In)elastic nuclear scattering

- chiral lattice EFT calculations for many nucleons are performed as Monte-Carlo simulations (instead of using Lanczos algorithm)

⇒ evolve Hamiltonian in Euclidean (i.e. Wick-rotated) time τ

⇒ evaluate matrix element $|\langle\psi_{\text{test}}|\exp(-\hat{H}\tau)|\psi_{\text{test}}\rangle|^2$ at different points in time to obtain spectral overlap function

- Lüscher's formula not accurate enough here because error of Monte-Carlo energy levels is larger than separation between these levels **[B.-N. Lu et al. (2016)]**

Outlook: (In)elastic nuclear scattering

- chiral lattice EFT calculations for many nucleons are performed as Monte-Carlo simulations (instead of using Lanczos algorithm)

$\Rightarrow$ evolve Hamiltonian in Euclidean (i.e. Wick-rotated) time τ

$\Rightarrow$ evaluate matrix element $|\langle\psi_{\text{test}}|\exp(-\hat{H}\tau)|\psi_{\text{test}}\rangle|^2$ at different points in time to obtain spectral overlap function

- Lüscher's formula not accurate enough here because error of Monte-Carlo energy levels is larger than separation between these levels **[B.-N. Lu et al. (2016)]**

- extension to inelastic scattering (not possible with Lüscher): use two-cluster state

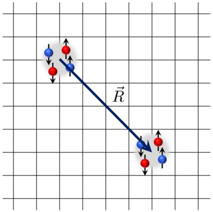

[S. Elhatisari et al. (2015)]

$$|\psi_{\text{test}}(\vec{R}\,)\rangle = \sum_{\vec{r}} |\vec{r}+\vec{R}\,\rangle_{\text{cluster 1}} \otimes |\vec{r}\,\rangle_{\text{cluster 2}}$$

$\Rightarrow$ interpret Breit-Wigner peak width Γ as decay rate of compound nucleus

Summary

- presented spectral overlap method for determining finite-continuum/lattice resonances
- several advantages compared to Lüscher's formula:
  - more reliable Breit-Wigner fit for small and coarse lattices
  - overlap has nearly no background like cross section
  - easy generalization for high orbital angular momenta and partial-wave mixing
  - suitable for chiral lattice EFT simulations of heavy nuclei
  - extendable to inelastic scattering
- additional work in progress:
  - 3D single-channel benchmark by C. Wang (Bochum, NLEFT collaboration)
  - realistic nuclear systems by A. Sarkar (Jülich, NLEFT collaboration)

Thank you for your attention!